Published in *Geotechnical Testing Journal* 43 (5) **2020**

Centrifuge modelling of the impact of local and global scour erosion on the monotonic lateral response of a monopile in sand

Li, Q.[a,1], Prendergast, L.J.[b,2], Askarinejad, A.[a,3,*], Chortis, G. [a,4], Gavin, K.[a,5]

[a] Faculty of Civil Engineering and Geosciences,
Delft University of Technology,
Building 23,
Stevinweg 1 / PO-box 5048,
2628 CN Delft / 2600 GA Delft,
The Netherlands

[b] Department of Civil Engineering,
Faculty of Engineering,
University of Nottingham,
Nottingham,
NG7 2RD,
United Kingdom

[*]Corresponding author

Email: [1]Q.Li-3@tudelft.nl, [2]luke.prendergast@nottingham.ac.uk, [3]A.Askarinejad@tudelft.nl, [4]G.Chortis@student.tudelft.nl, [5]k.g.gavin@tudelft.nl

Abstract

The majority of offshore wind turbines are founded on large-diameter, open-ended steel monopiles. Monopiles must resist lateral loads and overturning moments due to environmental (wind and wave) actions, while vertical loads tend to be comparatively small. Recent developments in turbine sizes and increases in hub heights have resulted in pile diameters increasing rapidly, whilst the embedment length to diameter ratio (*L*/*D)* is reducing. Soil erosion around piles, termed scour, changes the soil strength and stiffness properties and affects the system's load resistance characteristics. In practice, design scour depths of up to 1.3*D* are routinely assumed during the turbine lifetime, however the impact on monopiles with low *L/D* is not yet fully understood. In this paper, centrifuge tests are performed to assess the effect of scour on the performance of piles with low *L*/*D*. In particular, the effect of combined loads, scour type (global, local) and depth are considered. A loading system is

developed that enables application of realistic load eccentricity and combined vertical, horizontal and moment loading at the seabed level. An instrumented 1.8 m diameter pile with L/D = 5 is used. A friction-reducing ball-type connection is designed to transfer lateral loads to the pile without inducing any rotational pile-head constraint, associated with loading rigs in tests of this nature. Results suggest that vertical and lateral load interaction is minimal. Scour has a significant impact on the lateral load-bearing capacity and stiffness of the pile, leads to increases in bending moment magnitude along the pile shaft, and lowers the location of peak pile bending moment. The response varies with scour type, with global scour resulting in larger moments than local scour. The size of the local scour hole is found to have a significant impact on the pile response, suggesting that scour hole width should be explicitly considered in design.

Keywords: Centrifuge test; Scour; Monopile; Lateral response

1 Introduction

The majority of offshore wind turbines (OWTs) constructed to date are founded on monopile foundations. Developments in construction methods and improved design procedures (Byrne et al. 2015; Byrne et al. 2018) has resulted in a gain in market share for monopiles from approximately 75% of offshore wind turbine foundations in 2012 (Doherty and Gavin 2012) to more than 87% in 2017 (Wind Europe 2017). Monopiles are an efficient, cost effective, and proven technology to resist the large lateral loads and moments due to wind and wave actions, and thus provide a low-risk solution for offshore developers. Whilst all limit states are important, monopiles have strict serviceability requirements, e.g. total rotation at seabed level typically must remain less than 0.5° (Arany et al. 2017; Prendergast et al. 2018).

When structures are founded in water, there is potential for erosion of the supporting soils, a mechanism known as scour. Interested readers are referred to Wang et al. (2017) for a comprehensive review on scour in the context of bridges. For the present application, scour erosion around unprotected

offshore piles changes the support conditions and can pose a significant problem (Sørensen and Ibsen 2013; Prendergast et al. 2015). Scour increases the free cantilevered length of monopiles, leads to a reduction in the soil's effective stress, reducing the strength and stiffness of the remaining soil, and can thus compromise the serviceability and safety of structures (Hoffmans and Verheij 1997; Sumer and Fredsøe 2002). There are two main types of scour relevant to offshore structures, see Fig. 1: (i) 'global scour', where the elevation of the soil surface is reduced globally due to natural sea bed migration or the presence of a whole wind farm interfering with the global flow regime, and (ii) 'local scour', where the disturbed flow directly local to a pile structure leads to the formation of a conical scour pit around the foundation (Mostafa 2012). Global scour due to storm surge events has been reported in the literature (Robertson et al. 2007), with resulting scour depths of the order of 1*D* (*D* = pile outer diameter). The typical range for local scour depth, D_s, considered in design is 1.3*D*. It is noteworthy that in the marine environment, scour occurs due to the combination of tides, currents and waves, which can make the estimation of scour depths very difficult (Prendergast et al. 2015; Negro et al. 2014). Since monopiles have slenderness ratios (pile penetration normalised by pile diameter, *L*/*D*) of < 6, scour can have a major impact on the stiffness and capacity of these systems. Some previous works that have investigated the effect of scour on the lateral resistance characteristics of piles are discussed herein.

Bennett et al. (2009) examined the effect of scour and pile head boundary conditions on the lateral deflections of a pile group, used as the foundation for a bridge pier. The lateral behaviour was examined using the Group Equivalent Pile (GEP) method. Results showed that scour reduces the lateral capacity, which is especially significant when the scour depth exceeded the depth of the pile cap. Moreover, scour altered the influence depths of deflection, bending moment and shear, by lowering the point where the maximum value of these parameters occurred. Lin et al. (2010) investigated the influence of the change in stress history of sand due to scour on the lateral behaviour of piles by modifying soil reaction - lateral displacement (*p*-*y*) curves. They recognised that most scour analyses

simply remove upper layers of soil to simulate scour with no change in the properties of the remaining soil, and this ignores the fact that the remaining soil will have experienced different stress histories before and after scour. By comparing calculated results from the modified sand *p-y* curves against a referenced field test, they concluded that the change in the over-consolidation ratio due to scour had the most significant influence on the sand lateral resistance properties, and leads to higher resistance in the remaining sand. Ignoring this additional effect is conservative. A subsequent study by the same authors in Lin et al. (2016) presents a simplified method for the analysis of laterally loaded piles in soft clay using modified *p-y* curves to account for scour hole dimensions (scour depth, scour width, scour-hole slope angle). By comparing the results of their model with a 3D finite difference model (developed using FLAC3D), it was observed that ignoring the scour hole dimensions could result in 10-19% larger lateral displacement at the pile head with bending moments being 6-8% larger, as compared to the case where these are explicitly considered. Zhang et al. (2017) also recognised that soil stress history changes are typically ignored along with whole scour-hole geometry. They examined the behaviour of laterally loaded long-slender piles ($L/D \approx 40$) in soft clay under scoured conditions by using modified *p-y* curves to reflect the effects of three-dimensional scour-hole geometry (depth, width, and slope angle) as well as the stress history of the soil. The results indicated that neglecting the effect of soil stress history can be unconservative for pile foundations in soft clay affected by scour. Furthermore, neglecting the scour-hole geometry is over-conservative for design of laterally loaded piles under scour. For the purpose of design, the scour effect on the pile lateral behaviour may be characterised in terms of scour depth and the stress history of the soil. Further work by the same authors extended this approach to investigate the influence of vertical loads on the lateral responses of scoured piles, taking soil stress history and scour hole geometry into consideration (Liang et al., 2018). Mostafa (2012) investigated the influence of scour type (local and global) on the lateral response of piles in both cohesive and cohesionless soils using numerical modelling. The study concluded that scour had a more deleterious effect on piles installed in sand than in clay. In sand, scour depths ranging between

1*D* and 3*D* resulted in lateral pile head displacement increases of 37% to 155%, as compared to the no scour condition. Moreover, global scour caused large increases in bending moments with the result that scour had a more significant impact for piles subjected to large lateral loads due to nonlinear pile-soil interaction effects. Qi et al. (2016) investigated the effect of scour type (local and global) on *p*-*y* curves of piles for OWTs in sand using centrifuge testing. They found that, under global scour, the *p*-*y* curves in the remaining over-consolidated soil showed no obvious difference to those in the original normally consolidated soil. This finding is contradictory to the hypothesis in Lin et al. (2010). Furthermore, under local scour, they found that the remaining overburden provided a beneficial response in that the lateral soil stiffness at a given depth below the scour hole base was greater than at the same relative depth below the original mudline. The tests were performed using relatively flexible piles with a slenderness ratio between 9.5 and 12.5.

To date, there has been considerable research undertaken on the effect of scour on the lateral response characteristics of piles using numerical modelling or scaled laboratory testing. Limited research has been undertaken, however, on the effect of scour depth and type on laterally loaded piles considering combined vertical, lateral and moment loading at the seabed level using centrifuge testing, particularly for the piles with low slenderness ratios typically used for offshore wind developments. Moreover, the influence of local scour hole size has not received significant attention in physical modelling. This paper presents the development of a centrifuge-based model specially designed to study the effect of scour on laterally loaded monopiles with low slenderness ratios. The challenge lies with the application of lateral loads and moments in a centrifuge while minimizing the constraint on the pile head fixity (i.e. the pile head should be free to rotate as per an offshore monopile). Moreover, the presence of vertical dead loading representing the self-weight of an OWT should be considered. This paper details the development of the testing arrangement in the Geo-Engineering laboratory at Delft University of Technology (TU Delft) and investigates lateral load-displacement responses and derived bending moment distributions of an instrumented pile under global scour, and two types of local scour. The

two types of local scour, termed narrow and wide in this paper, refer to the bottom width of the scour hole, where W_b = 0 for narrow scour, and W_b = D for wide scour (see Fig. 1).

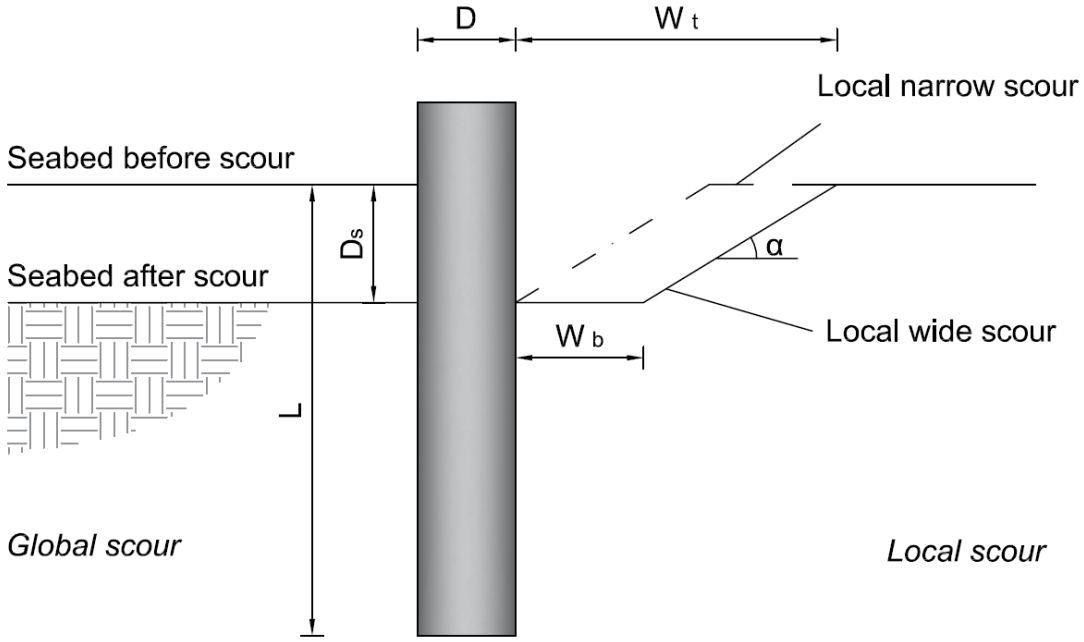

Fig. 1 Schematic of local and global scour. w_b = bottom width of scour hole; w_t = top width of scour hole; α = scour slope angle; L = original embedment length; D = diameter; D_s = scour depth.

2 Centrifuge modelling of scoured piles under monotonic lateral loading

2.1 Centrifuge facility

The TU Delft centrifuge, see Fig. 2, is a 2m diameter beam-type apparatus (Allersma 1994). Centrifuge tests are performed on models that are geometrically N-times smaller than a prototype. The geo-centrifuge provides a unique environment of enhanced gravitational acceleration (N*g*), where the expected behaviour of a full-scale geotechnical structure can be observed, with high precision, using small-scale models. The centrifuge at TU Delft enables models with dimensions up to 300 mm × 400 mm × 450 mm be tested up to a maximum of 300 times the gravitational acceleration (300*g*). While

this is possible, for practical reasons related to the operation of the data logging equipment, samples are typically tested at a limiting gravitation acceleration of 100*g*.

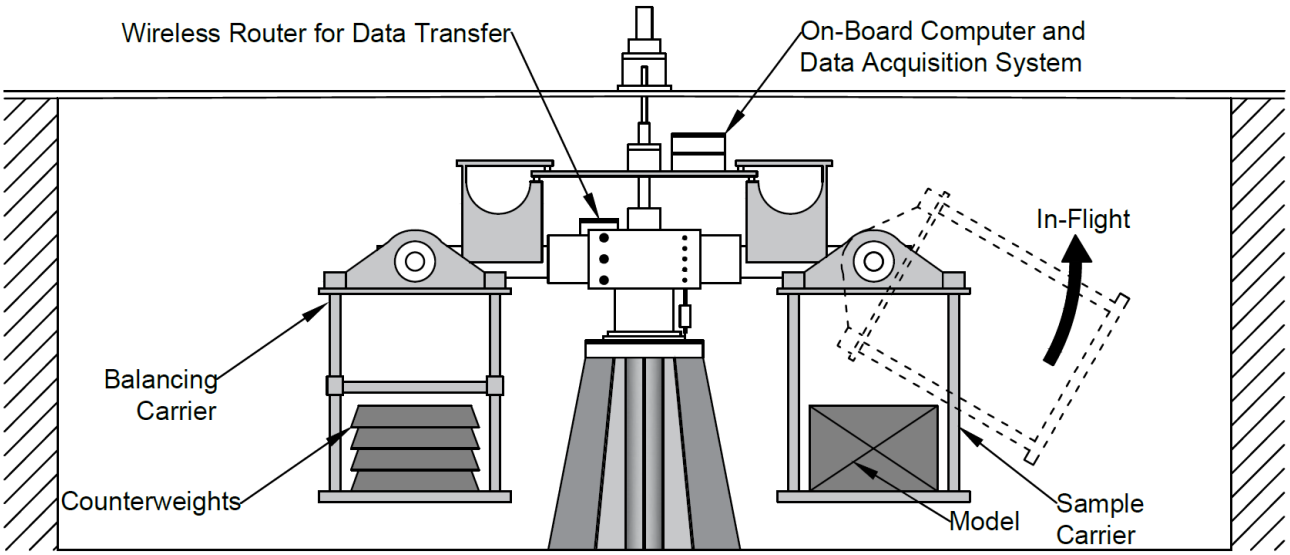

Fig. 2 Schematic layout of the geo-centrifuge at TU Delft

For simulating geotechnical structures using a centrifuge, scaling laws must be considered. Table 1 provides a summary of typical scaling laws for modelling of pile-type structures. In this table, N refers to the gravitational acceleration field adopted in a given test.

Table 1. Basic scaling laws for centrifuge modelling of monopiles

Term [Dimension]	Prototype	Model
Length (Pile diameter, Length) [L]	1	1/N
Second moment of area [L^4]	1	$1/N^4$
Flexural stiffness [ML^3/T^2]	1	$1/N^4$
Mass [M]	1	$1/N^3$
Force [ML/T^2]	1	$1/N^2$
Stress [$M/(LT^2)$]	1	1
Strain [-]	1	1

2.2 Model pile

The model pile is an open-ended cylindrical aluminium tube with an outer diameter (D) of 18 mm (see Fig. 3). The pile diameter is selected so as to minimise boundary effects associated with the strong box, which houses the pile, and also to satisfy constraints associated with the mean grain particle size (see section 2.4). The strong box is fabricated from bolted plexiglas with dimensions 410 (length) × 150 (width) × 180 (height) mm^3, see Figs. 4 and 5. The pile has a total length of 240 mm and is embedded 90 mm into the sand. The embedded depth is chosen so as to model a pile with slenderness ratio (L/D) between 4-6 (Sørensen and Ibsen 2013; Doherty and Gavin 2012; LeBlanc et al. 2010), within the typical range for offshore monopiles. A pile with embedded length of 90mm equates to a slenderness ratio of 5. The wall thickness of the model pile is derived based on the calculations for minimum wall thickness for monopiles (API 2007; Arany et al. 2017). Using the similitude between the flexural rigidity (EI) of the prototype and the model (Table 1), the wall thickness is calculated to be 1mm at model scale. Byrne et al. (2015) have produced a database of piles, and present the results of pile diameters normalised by pile wall thickness. For monopiles with L/D = 5, the value of D/t varied from 39 to 80. In the present analysis, the D/t value for the steel prototype pile is 60, which is within the expected range.

The pile was installed for each test by jacking in place at 1g prior to initiating the centrifuge. It should be noted that installing the model pile at 1g equates to an idealised 'wished-in-place' treatment, and does not consider the potential residual base stresses that might be developed if driven while the centrifuge is in flight. These residual stresses may lead to additional base moments on the piles (Murphy et al. 2018), which may alter the response characteristics. Moreover, installation of the pile at 1g results in shearing along the shaft at lower confining stresses compared to in-flight installation. This condition promotes dilative behaviour of the sand at the shear band. However, since medium dense sand with a relative density of 53% is used in the present study, significant dilative behaviour is not expected. Furthermore, driving the pile at Ng would require stopping of the centrifuge to adjust

184 the loading rig for the subsequent lateral load application, which would add uncertainty surrounding
185 the influence of the sample stress history on the results obtained. The present paper ignores the
186 influence of installation effects.

187 All load tests were performed at 100*g*, therefore, the model pile properties correspond to a 1.8 m
188 diameter rigid structure, with a wall thickness of 30 mm, an embedment of 9 m and a total length of
189 24 m at the prototype scale. The primary dimensions and material properties of the pile are provided
190 in Table 2.

191 Ten strain-gauge pairs are installed along the pile shaft to enable the distribution of bending moments
192 due to the applied loading be derived. The strain gauges used are FLA-3-11 fabricated by Tokyo Sokki
193 Kenkyujo (Tokyo Sokki Kenkyujo 2018). Of these 10 gauges, 7 may be logged simultaneously during
194 testing, due to a limitation in the available channels of the data acquisition system. In each analysis
195 case conducted, the most appropriate seven gauges are used. The load from the superstructure is
196 incorporated by way of adding steel blocks with equivalent (prototype) weight of 3MN, to the pile top.
197 The masses were fabricated from quadrate steel with an outer length of dimension 50 mm and a
198 thickness of 12 mm. In the centre of each mass is a circular hole with a diameter of 18 mm to allow
199 the masses be fixed on the pile body (see Fig. 3).

200 Table 2 Model and corresponding prototype pile dimensions and properties

Property	**Model pile**	**Prototype pile****
Length (embedded + additional)	90 + 150 mm	9 + 15 m
Diameter, outer	18 mm	1.8 m
Wall thickness	1 mm	30 mm *
Young's modulus (E)	70 GPa	210 GPa *
Moment of inertia (I)	1936 mm^4	0.065 m^4
Flexural stiffness (EI)	0.137 $kPa.m^4$	13.7 $GPa.m^4$

201 *Assume prototype pile is fabricated from steel
202 **N = 100 adopted in present study

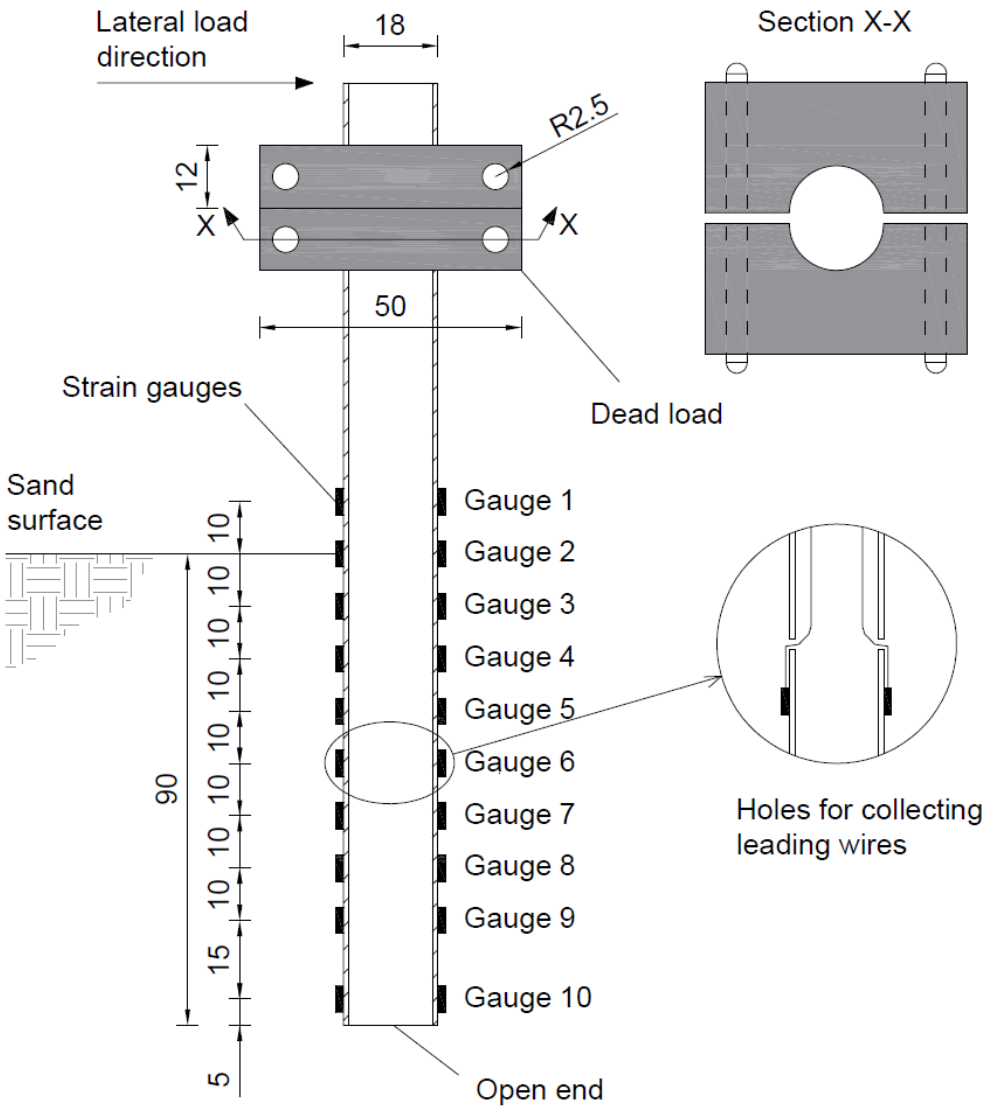

Fig. 3 Model pile schematic diagram with strain gauge layout (dimensions in mm)

2.3 Loading system for pile model

The tests in this study were performed at 100*g* to model a rigid monopile with a diameter of 1.8 m (at prototype scale) and *L*/*D* of 5. A two-dimensional servo actuator applies loading to the pile head, as shown in Figs. 4 and 5. The loading system is capable of applying lateral loads under either load or displacement controlled conditions. The vertical dead load (*V*) at the pile head can be imposed by means of attaching steel blocks with different masses, to model the presence of a superstructure (details

of the dead load are described in section 2.2). The lateral load (L) is applied at the pile head by lateral movement of the actuator, and is monitored by strain gauges located on the loading arm. The lateral displacements of the pile at the loading position (pile head) can be monitored by the lateral motor encoders, the accuracy of which are of the order of approximately 3×10^{-5} mm. For all tests performed in this study, lateral loads are applied at a height of 15 m above the seabed at prototype scale.

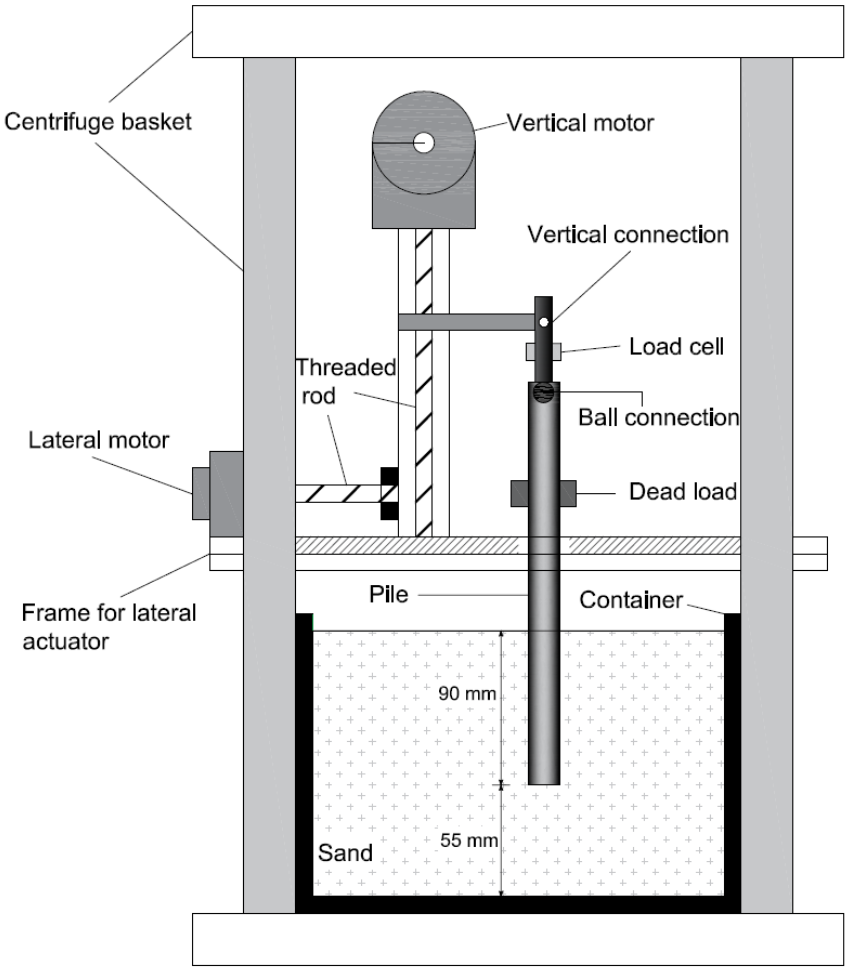

Fig. 4 Schematic of two-dimensional loading actuator and monopile arrangement in centrifuge tests

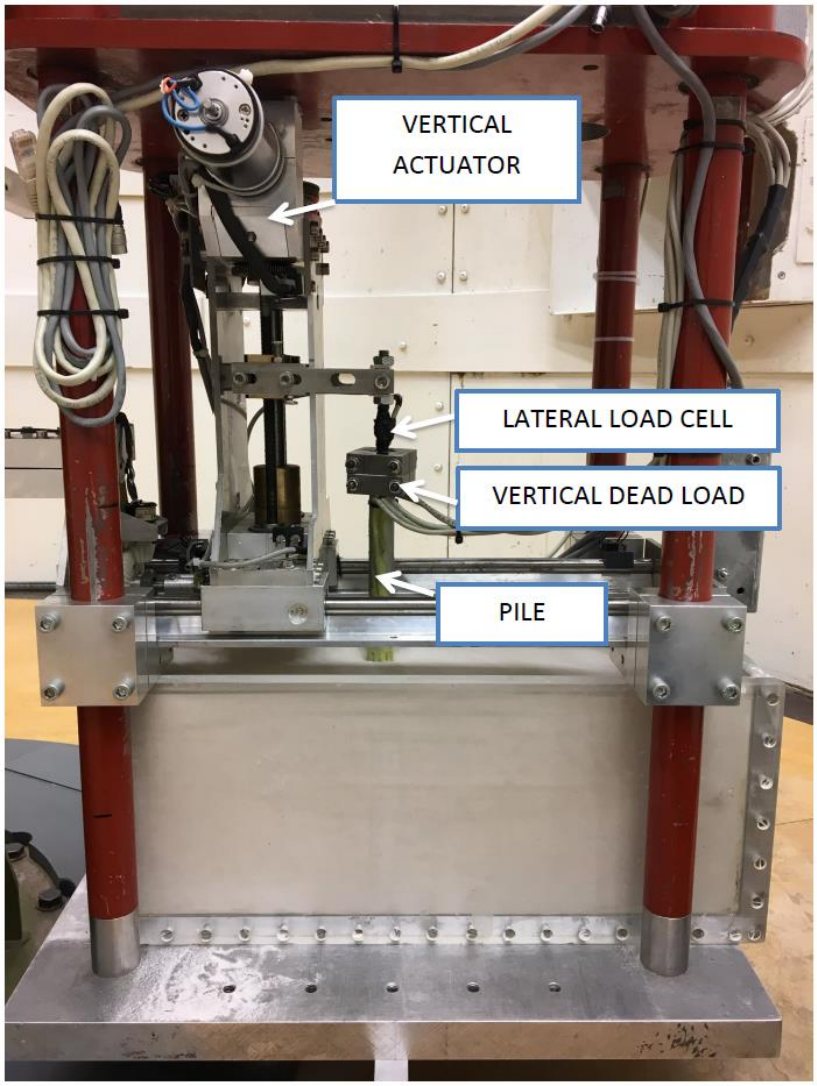

Fig. 5 Picture of pile testing arrangement

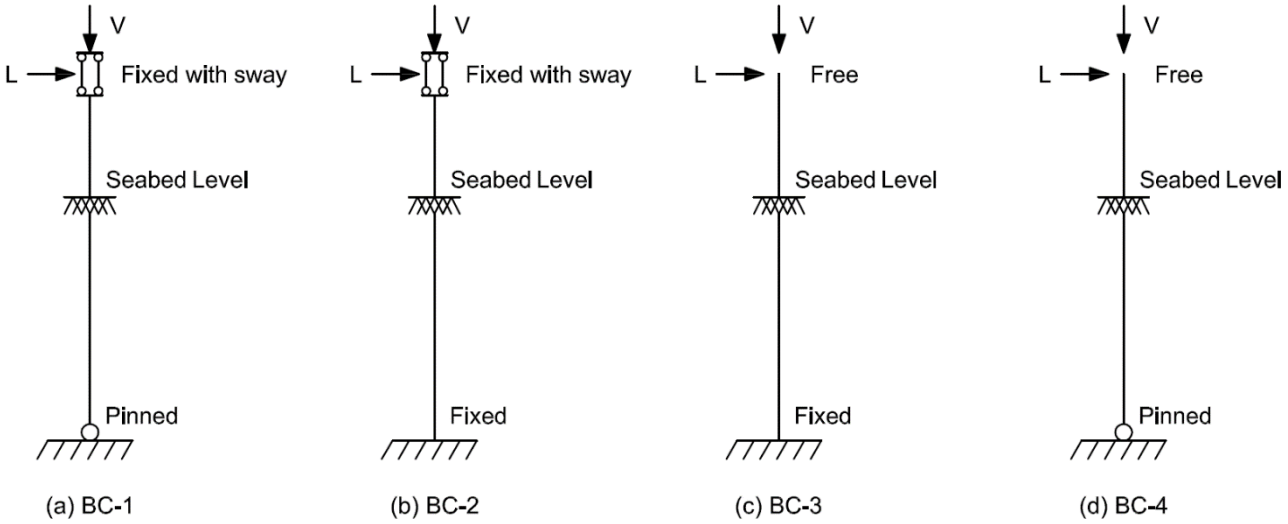

Fig. 6 Different boundary conditions for laterally loaded piles (after Han & Frost 2000), (a) head fixed against rotation with pile tip seated on hard soil; (b) head fixed against rotation with pile tip embedded in hard soil; (c) head free and pile tip embedded in hard soil; (d) head free with pile tip seated on hard soil.

Han and Frost (2000) recognized that the load-deflection response of a laterally loaded pile is highly dependent on the boundary conditions of the pile in the ground. Various boundary conditions for piles are encountered in practice, and four typical scenarios are shown in Fig. 6. Monopiles for offshore wind turbines will typically behave similarly to BC-4 (with some additional pile tip sway). Achieving the free head boundary condition in centrifuge tests is difficult, therefore most previous research tends to only consider lateral movement of the pile head (by implementing a roller-type connection) while ignoring any pile head rotation (BC-1 and BC-2).

To enable the application of a lateral load without inducing any rotational fixity associated with the loading arm, a specially-designed friction-reducing ball connection (shown in Fig. 7) was constructed to transfer the lateral loading produced by a linear actuator to the pile head. The ball is placed vertically into the open-end of the pile head, where it rests in contact with the internal shaft of the pile. A Teflon

239 sleeve is used to minimize the interface friction between the ball and the pile internal surface. Fig. 7
240 shows a photograph of the ball connection used in this study and Fig. 8 shows the instrumented model
241 pile with Teflon interior at the top, and the shielded strain gauges along the shaft.

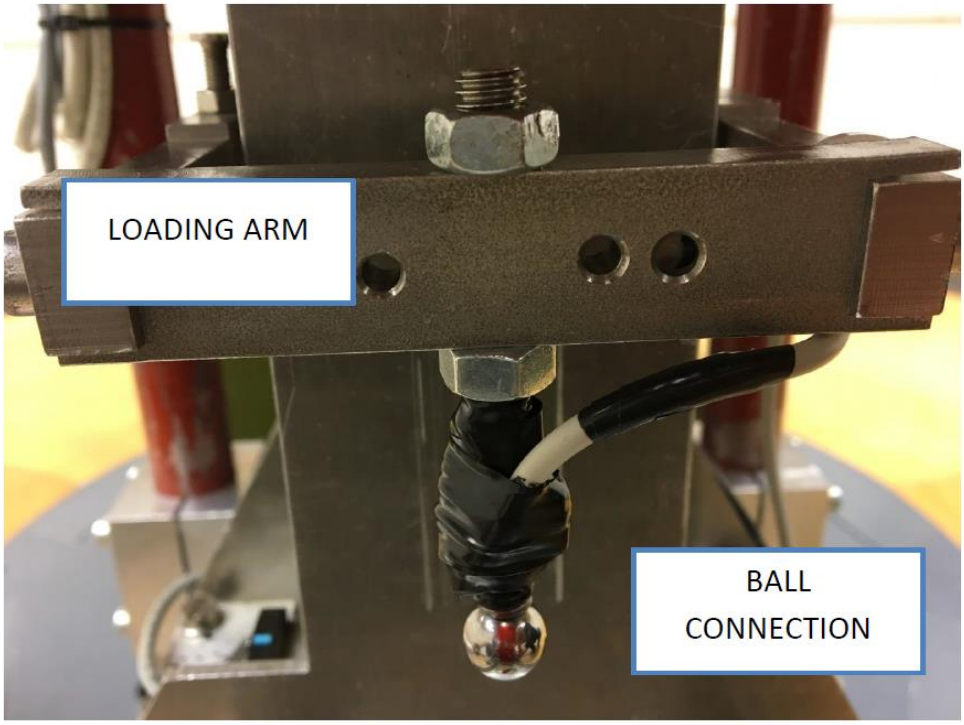

242

243 Fig. 7 Ball connection for reduced friction application of lateral load

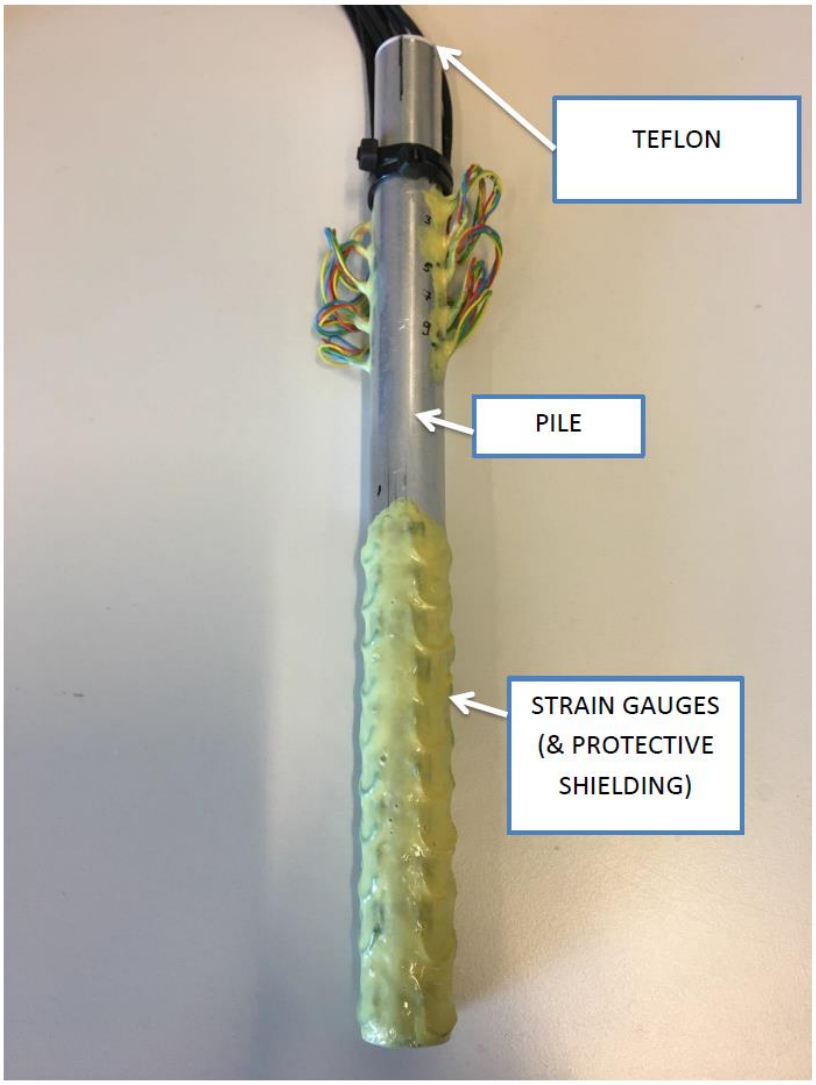

Fig. 8 Pile with inner Teflon material for reduced friction

2.4 Soil preparation and characterisation

Fine, uniform Geba sand (SibelcoEurope 2016) was used in this study. It is mainly comprised of silica (99% SiO_2) and 84.2% of the grains have a diameter between 0.1 mm and 0.2 mm. The ratio of pile diameter to average grain size of the sands (D/D_{50}) for the tests is approximately 164, which is larger than the value of 20 and 60 suggested by Gui et al. (1998) and Remaud (1999), where grain size effects become negligible for laterally loaded piles (Garnier et al. 2007; Nunez et al. 1988). A relative density (D_r) of 53% was adopted for the prepared sand used in the experiments conducted in this paper. The

main properties are summarised in Table 3. No water was considered in the experimental trials conducted in this paper. It should be noted that while this is a simplification and a deviation from the physical reality of scoured offshore piles, the presence of water is not expected to alter the observed behavioural trends, rather its presence would lower the effective unit weight of the sand. A similar treatment can be observed in Mu et al. (2018); Verdure et al. (2003); Klinkvort and Hededal (2013); LeBlanc et al. (2010); and Li et al. (2010).

Table 3 Basic soil properties of Geba sand (De Jager et al. 2017; Maghsoudloo et al. 2018)

Property	**Sand**
Group Symbol Based on USCS[a]	SP
Median Particle Size, D_{50} (mm)	0.11
Curvature Coefficient, C_C	1.24
Uniformity Coefficient, C_U	1.55
Specific Gravity, G_S	2.67
Plasticity Index, PI	NP
Maximum Void Ratio, e_{max}	1.07
Minimum Void Ratio, e_{min}	0.64

[a]Unified Soil Classification System (USCS) (ASTM D2487).

2.5 Scour hole excavation

In order to study the effect of different types of scour erosion, it is necessary to develop a method to model scour hole geometries in the centrifuge. To cover the main range of expected scour hole geometries, three different scour hole shapes (one for global scour and two for local scour) were considered, see Fig. 1. Fig. 1 shows a schematic of simplified global and local scour. In the models, D denotes pile diameter, W_t denotes top width of scour hole, W_b denotes bottom width of scour hole, D_s denotes scour depth and α denotes slope angle of the scour hole. A range of scour depths of 1D, 1.5D and 2D were implemented in this study to cover the ranges considered by Kishore et al. (2008); Sumer et al. (1992); Sumer et al. (2007); and Det Norske Veritas (2011). Global scour was modelled through the complete removal of a given soil layer, see Fig. 1, and typically occurs due to natural seabed

migration. Local scour represents the case of a scour hole forming in the direct vicinity of a pile. To model local scour, a scour hole was created in the shape of an inverted frustum. To investigate the influence of scour hole size, the scour hole base extends around the pile at a distance (W_b) varying between 0 and D. A scour hole with a base width $W_b = 0$ is termed *local narrow scour* while a scour hole with a base width $W_b = D$ is termed *local wide scour* in subsequent analyses in this paper. A scour hole side slope of 30° was adopted for all cases, which is in line with previous experiments (Roulund et al. 2005; Hoffmans and Verheij 1997). Note, the scour side slope angle is the least important factor among the three scour hole dimensions (scour depth, scour width, scour-hole slope angle) influencing the responses of laterally loaded piles (Li et al. 2013; Zhang et al. 2017). For this reason, it is kept constant in the present study.

To excavate sand to form the scour hole types described, rigid moulds were fabricated, as shown schematically in Fig. 9. These moulds, with varying depths and base widths were used to ensure the shape of the scour holes adhered to the required dimensions for each test. Each scour hole was created immediately prior to jacking the model pile at 1g and just before spinning the centrifuge up to 100g.

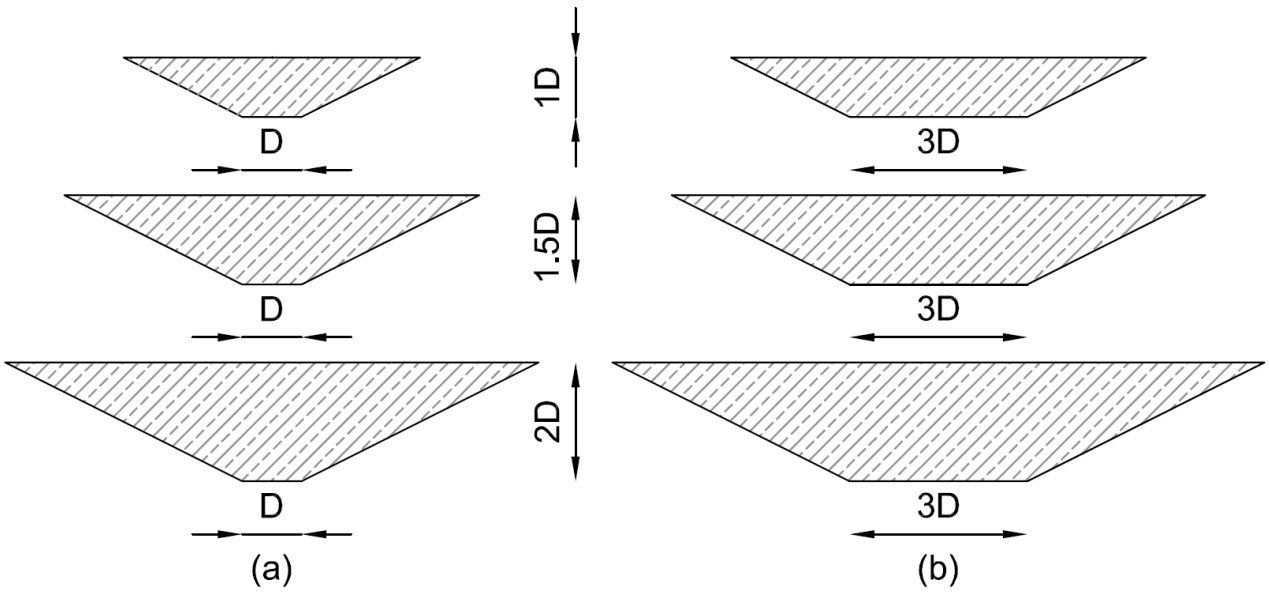

Fig. 9 Schematics of (a) scour hole moulds of local narrow scour and (b) scour hole moulds of local wide scour

290 ## 2.6 Testing Program

291 Displacement controlled lateral loading is applied to the pile head by the lateral movement of the
292 actuator at a constant displacement rate of 0.01 mm/s. Each test continues until the loading arm reaches
293 the target displacement. The testing program comprised investigating the effect of scour depth and
294 scour type on the lateral behaviour of the pile (capacity and bending moment). No scour, and three
295 scour depths equating to 1*D*, 1.5*D* and 2*D*, were studied. Moreover, three scour types, namely local
296 narrow scour, local wide scour and global scour were also investigated to ascertain the influence of
297 scour hole size (overburden dependency) on the pile lateral behaviour. Each test was undertaken twice
298 to ensure repeatability. A constant vertical load of 3MN was applied to represent the weight of a
299 superstructure. The testing program is summarised in Table 4.

300 Table 4 Programme of centrifuge test

Test number	**Scour type**	**Scour depth**	**Vertical dead load at prototype scale (MN)**	**Description**
1	No scour	-	0, 1.5 and 3	Zero scour lateral load test
2	Global scour	1D	3	Scour test
3	Global scour	1.5D	3	Scour test
4	Global scour	2D	3	Scour test
5	Local wide scour	1D	3	Scour test
6	Local wide scour	1.5D	3	Scour test
7	Local wide scour	2D	3	Scour test
8	Local narrow scour	1D	3	Scour test
9	Local narrow scour	1.5D	3	Scour test
10	Local narrow scour	2D	3	Scour test

301

302

303 # 3 Results and discussion

304 The load-displacement response and bending moment profiles of the piles under various scour
305 conditions are reported in this section.

3.1 Lateral load-displacement and bending moments under zero scour condition

The pile head load-displacement response measured for the no-scour base-case condition is shown in Fig. 10 (Test 1). The ultimate lateral resistance of a pile is usually defined as a displacement equal to 10% of the pile diameter, $H_{0.1}$, at the seabed (mudline) level. In the present study, the pile head displacement (as opposed to the seabed displacement), is the measured parameter, which is 15m above the seabed level (at the prototype scale). For the purpose of comparison of the scour cases considered in this paper, the ultimate resistance, H_{ult}, is defined as a pile head displacement of 1 pile diameter, in this case 1.8m. In Fig. 10, the pile is loaded up to and beyond the specified ultimate resistance, and it can be seen that the lateral resistance continues to increase to a value of 970 kN at a lateral pile-head displacement of 3m (Fig. 10a). The presence of a vertical load (superstructure weight) had a minimal effect on the lateral response for this pile geometry with the H_{ult} capacity changing by approximately 1% as the vertical applied load increased from 0 to 3 MN. As a result, all remaining tests were performed with a 3 MN vertical load to represent the superstructure weight.

Fig. 10(b) shows the bending moments derived from the strain gauge readings using 7 of the 10 strain gauge pairs for the applied loading in Fig. 10(a). As discussed earlier, because of limitations with the data logger, only seven strain gauge pairs could be analysed at any one time. Bending moments are derived from bending strain measurements using Eq. (1).

$$M(z) = EI\rho(z) \tag{1}$$

where *EI* is the flexural rigidity of the pile and ρ(z) is the curvature at a given applied load, obtained as the ratio between the difference in measured compressive and tensile strains to the gauge lever arm (pile diameter) at a given depth *z*. The absolute values of the bending moments derived from each of the strain gauges shows an increasing trend with increased lateral displacement. In order to understand the evolution in the relative magnitudes of these bending moments along the pile, these are better viewed by plotting the values of bending moment at a given depth along the pile as a function of the

pile head displacement. This is undertaken in Fig. 10(c), which shows the evolution in bending moment profiles along the pile as the lateral pile head deflection (h) increased from 0.5m to 3m. As is evident, the shape of the bending moment profile is broadly conserved for increasing pile displacements, and the peak bending moment occurs at approximately the same depth in each case (between -2m and -3m below ground level, bgl).

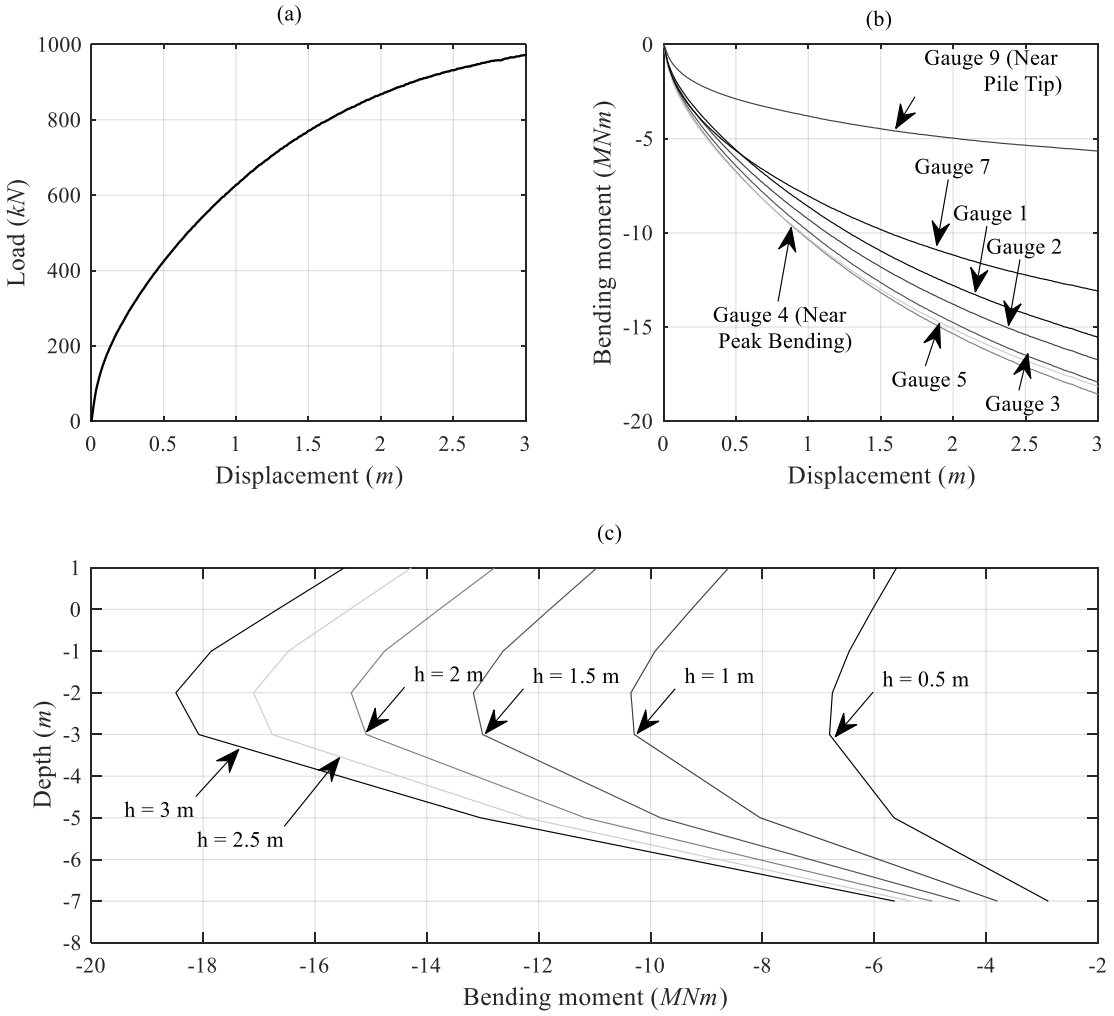

Fig. 10 Zero scour response features from centrifuge testing at prototype scale, (a) Pile head lateral load-displacement response, (b) Bending moment measurements along the pile, (c) Bending moment profiles for different levels of pile head displacement (h).

340 **3.2 Effect of scour depth on the lateral pile response**

341 The impact of four different local scour depths are investigated in this section, namely zero scour, and
342 scour with depths 1*D*, 1.5*D* and 2*D*. Only the results for a single scour type, namely local wide scour,
343 is considered. For this scour hole type, sand is removed up to a distance of 1*D* from around the pile.
344 The influence of scour size is investigated in a subsequent section.

345 The impact of increasing scour depth on the pile head lateral load-displacement responses is shown in
346 Fig. 11(a). For the cases considered, the H_{ult} value reduces from 831 kN to 234 kN as the scour depth
347 increases to 2*D*, a reduction of almost 72%. This result corroborates the findings in Lin et al. (2016),
348 which stated that scour depth is the most critical factor influencing the lateral behaviour of piles.

349 The bending moment distributions under 0, 1*D*, 1.5*D* and 2*D* scour are reported in Fig. 11(b), for an
350 applied lateral pile head load of 100 kN. As the scour depth increases, the absolute value of peak
351 bending moment M_{max} increases from 1.527 MNm for zero scour, to 1.615 MNm for 1*D* scour, to
352 1.711 MNm for 1.5*D* scour, to 1.86 MNm for 2*D* scour. This represents a change in peak bending
353 moment of 5.8%, 12.1% and 21.8% relative to the no-scour case for 1*D*, 1.5*D* and 2*D* scour
354 respectively. Furthermore, the location of the maximum bending moment also moves progressively
355 down the pile as scour depth increases, moving from -3m bgl to -5m bgl. These findings are in line
356 with previous research (Bennett et al. 2009), where the influence depth is observed to increase.

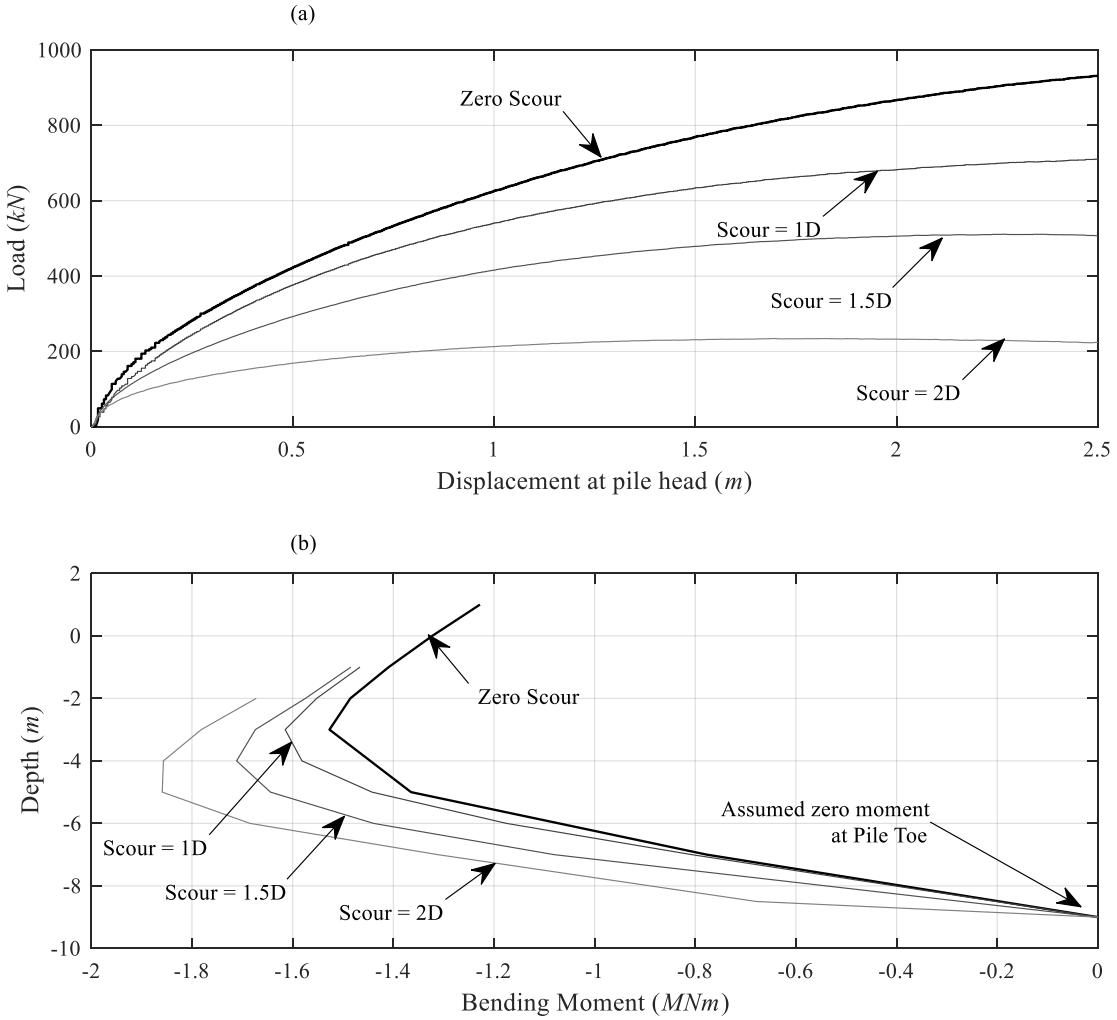

357

358 Fig. 11 Effect of scour depth on pile response characteristics at prototype scale, (a) Lateral load-
359 displacement response under increasing local wide scour, (b) Bending moment derived from strains
360 for increasing scour.

361

362 **3.3 Effect of scour type on the pile lateral response**

363 In this section, the effect of the scour type on the bending moment distribution along the pile under
364 scour is investigated. Local narrow, local wide and global scour types are compared with a view to
365 ascertaining if the scour hole size and associated overburden influence has an effect on the resulting
366 bending moment distribution. Fig. 12(a) shows the bending moment distribution measured along the

pile under a scour depth of 1*D*, for the three scour types, due to an applied lateral load of 100 kN at the pile head. Similar to previously, the absolute value of the bending moment profile increases between zero scour and 1*D* scour. Evidently, there is a difference between the local scour and global scour bending moment profiles, in that the global scour profile results in larger absolute values of bending moment under the applied load than the local scour profiles. For the scour depth of 1*D* (Fig. 12a), both local narrow and local wide scour exhibit similar bending moment profiles, suggesting that for this scour depth, there is negligible difference due to the variation in overburden pressure between both local scour widths. The maximum bending moment M_{max} increases 5.8% from the no scour case to the local scour cases, and 10.7% from the no scour case to the global scour case. It is interesting to note that the percentage change in peak bending moment between no scour and global scour for a depth of 1*D* (10.7%, Fig. 12a) is almost the same as the percentage change from no scour to local wide scour with a depth of 1.5*D* (12.1%, Fig. 11b), as discussed in section 3.2. While scour depth is still the most influencing factor for laterally loaded piles, this finding suggests that the overburden influence is quite important nonetheless. The location of the point of maximum moment reduces from -3m to -4m bgl, which suggests that the additional loss in overburden for the case of global scour relative to local scour forces the pile to mobilise resistance from a deeper depth of soil, in order to compensate for the loss of strength of the remaining soil.

Fig. 12(b) shows the same information as Fig. 12(a), but for a scour depth of 2*D*. In this case, there is a clear increase in the absolute magnitude of the bending moment profiles measured between no scour and the three scour types. This suggests that soil close to the pile in the narrow scour case provides enhanced effective confining stiffness, due to the presence of the remaining overburden. M_{max} increases 12.5% from the no scour to local narrow scour case, 21.7% to the local wide scour case, and 34.4% to the global scour case. The location of the point of maximum moment reduces from -3m to -5m below seabed level, as the soil seeks to balance the external loads by mobilising deeper soils to compensate for the overburden differences as discussed above. The influence of scour hole width is a

significant finding as many previous researchers completely ignore this effect, and simplify scour as the increase in free length of a structural element, without due attention to the properties of the remaining soil (Li et al. 2017; Prendergast et al. 2016). The physical modelling results in this paper highlight that this influence should not be discounted.

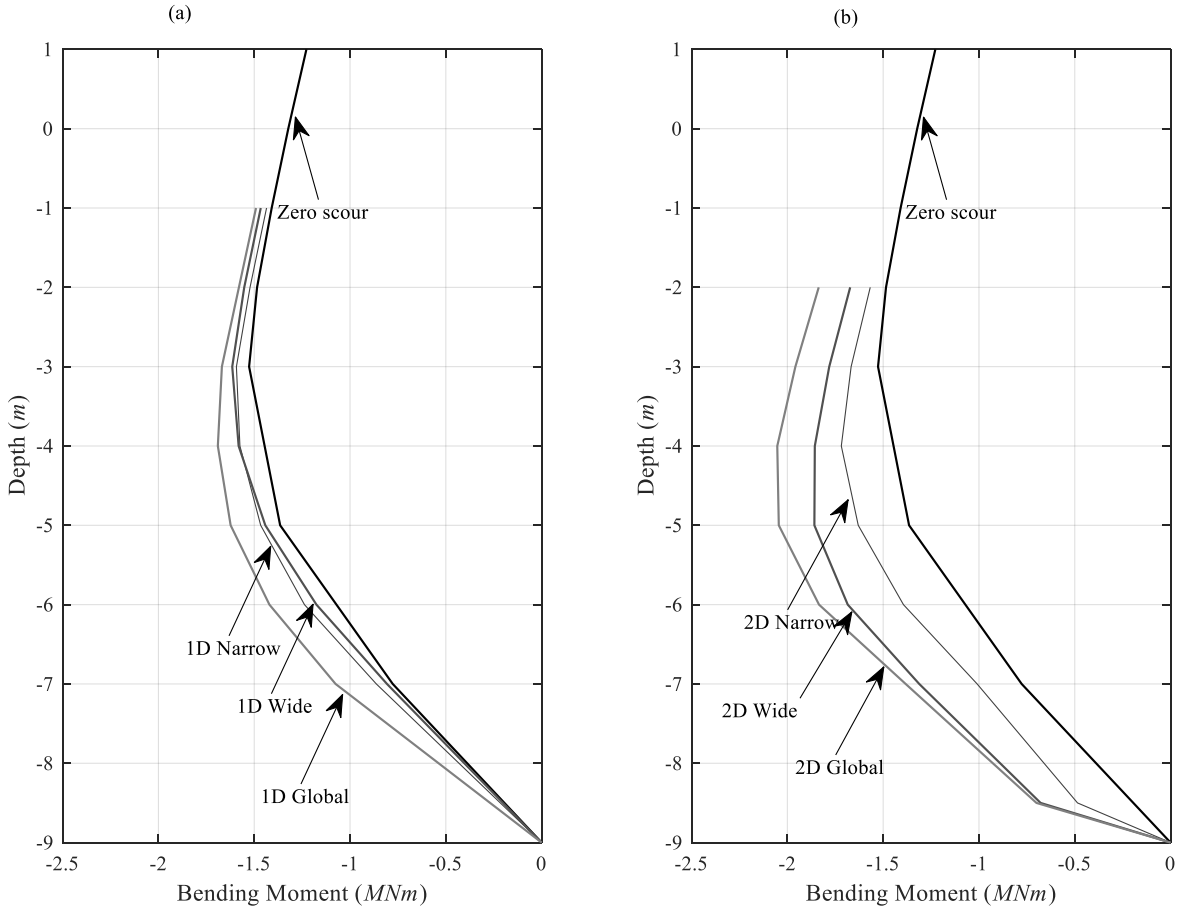

Fig. 12 Effect of scour type on bending moments measured along pile for applied lateral load = 100 kN, at prototype scale (a) Bending moments for narrow, wide and global scour to depth 1*D*, (b) Bending moments for narrow, wide and global scour to depth 2*D*.

4 Conclusions

This paper presents the development of a specially designed pile lateral loading system for centrifuge model tests that minimises the pile-head rotational constraint associated with tests of this nature. A

404 modelling scheme to evaluate lateral pile behaviour under combined lateral and moment loading at the
405 seabed level, under various scour conditions, is undertaken using this ball-type loading system. The
406 research is applicable to offshore monopiles with low slenderness ratios, used to support wind turbines.
407 The study has several conclusions:

408 • The friction-reducing ball connection with Teflon interface is adept at providing a lateral
409 monotonic load, with significantly reduced pile-head rotational fixity. This is useful for
410 research on offshore monopile models, which have a free head condition. Other types of
411 loading rigs, which use pin-type connections, have a tendency to apply a component of vertical
412 loading to pile models as lateral displacements become large. The ball-type connection adopted
413 in this study mitigates this issue.

414 • Scour reduces the lateral bearing capacity and stiffness of pile foundations and leads to
415 increased bending moments along the pile under similar lateral loads applied at the pile head.
416 Moreover, the location of the maximum bending moment occurs lower along the pile for
417 increased scour, which may have implications for the design of monopiles with variable wall
418 thickness. Increased pile wall thickness may be adopted in the region near surface soils to
419 increase bending resistance locally, therefore changes in the response regime due to scour has
420 potential design ramifications, and should be considered.

421 • In addition to scour reducing lateral capacity, the width of the scour hole has a noticeable effect
422 on the measured bending moments. For a scour depth of 1*D*, there is a distinct increase in the
423 bending moments for the case of global scour compared to local scour. However, little
424 difference is observed between both local narrow and local wide scour at this scour depth. For
425 the case of scour up to a depth of 2*D*, however, there is a significant difference between the
426 bending moments measured for each scour type, with the bending moment consistently
427 increasing from the no scour case to local narrow scour, to local wide scour and on to global

scour. This finding suggests that designers should explicitly consider scour hole geometry in design (at least in a preliminary capacity), as it is conservative to assume the entire soil layer is removed during scour. For local scour, the overburden close to the pile provides additional resistance to the remaining soil, reducing the bending moments relative to global scour.

This paper presented the background to the centrifuge-based analysis regime for a pile under various scour conditions. It should be noted that installation effects were not considered since the model piles were jacked into the soil at 1*g* prior to testing. If the piles were driven while in-flight, this would lead to the generation of residual base stresses, and potential moments at the pile base. While the analysis in this paper does not consider the presence of these additional base moments, the behavioural trends identified in this paper should be not affected. Further studies will expand the investigation to the influence of scour on soil reaction-lateral displacement *p-y* curves for piles with low slenderness ratios.

Acknowledgements

This work is partly funded by the Section of Geo-Engineering of Delft University of Technology. The first author has been funded by the China Scholarship Council (CSC). The second author wishes to acknowledge the Faculty of Engineering, University of Nottingham, for financial support received to facilitate this collaboration.

References

Allersma, H. G. B. 1994. “The University of Delft Geotechnical Centrifuge.” In *Centrifuge 94*, 47–52. Rotterdam.

API. 2007. “RP2A: Recommended Practice for Planning, Designing and Constructing Offshore Platforms - Working Stress Design.” Washington, DC.

Arany, L., Bhattacharya, S., Macdonald, J., and Hogan, S. J. 2017. “Design of Monopiles for

Offshore Wind Turbines in 10 Steps." *Soil Dynamics and Earthquake Engineering* 92: 126–52. https://doi.org/10.1016/j.soildyn.2016.09.024.

Bennett, C. R., Lin, C., Parsons, R., and Han, J. 2009. "Evaluation of Behavior of a Laterally Loaded Bridge Pile Group under Scour Conditions." In *Structures Congress 2009: Don't Mess with Structural Engineers: Expanding Our Role*.

Byrne, B. W., McAdam, R., Burd, H. J., Houlsby, G. T., Martin, C. M., Zdravković, L., Taborda, D. M. G., Potts, D. M., Jardine, R. J., Sideri, M., Schroeder, F. C., Gavin, K., Doherty, P., Igoe, D., Muir Wood, A., Kallehave D., Skov Gretlund, J. 2015. "New Design Methods for Large Diameter Piles under Lateral Loading for Offshore Wind Applications." In *International Symposium on Frontiers in Offshore Geotechnics*, 705–10. Oslo.

Byrne, B. W., McAdam, R. A., Burd, H. J., Houlsby, G. T., Martin, C. M., Gavin, K., Doherty, P., Igoe, D., Zdravković, L., Taborda, D. M. G., Potts, D. M., Jardine, R. J., Sideri, M., Schroeder, F. C., Muir Wood, A., Kallehave, D., Skov Gretlund, J. 2015. "Field Testing of Large Diameter Piles under Lateral Loading for Offshore Wind Applications." In *Proceedings of the XVI ECSMGE Geotechnical Engineering for Infrastructure and Development*, 1255–60. https://doi.org/10.1680/ecsmge.60678.

Byrne, T., Gavin, K., Prendergast, L. J., Cachim, P., Doherty, P., and Chenicheri Pulukul, S. 2018. "Performance of CPT-Based Methods to Assess Monopile Driveability in North Sea Sands." *Ocean Engineering* 166: 76–91. https://doi.org/10.1016/j.oceaneng.2018.08.010.

De Jager, R. R., Maghsoudloo, A., Askarinejad, A., and Molenkamp, F. 2017. "Preliminary Results of Instrumented Laboratory Flow Slides." In *1st International Conference on the Material Point Method*. Delft, Netherlands: Elsevier Ltd.

Det Norske Veritas. 2011. "DNV Offshore Standard DNV-OS-J101 Design of Offshore Wind Turbine Structures."

475 Doherty, P., and Gavin, K. 2012. “Laterally Loaded Monopile Design for Offshore Wind Farms.”
476 *Proceedings of the ICE - Energy* 165 (1): 7–17. https://doi.org/10.1680/ener.11.00003.

477 Garnier, J., Gaudin, C., Springman, S., Culligan, P., Goodings, D., Konig, D., Kutter, B., Phillips, R.,
478 Randolph, M., and Thorel, L. 2007. “Catalogue of Scaling Laws and Similitude Questions in
479 Geotechnical Centrifuge Modelling.” *International Journal of Physical Modelling in*
480 *Geotechnics* 7 (3).

481 Gui, M., Bolton, M., Garnier, J., Corte, J., Bagge, G., Laue, J., and Renzi, R. 1998. “Guidelines for
482 Cone Penetration Tests in Sand.” *Centrifuge* 98: 155–60.

483 Han, J., and Frost, J. 2000. “Load–Deflection Response of Transversely Isotropic Piles under Lateral
484 Loads.” *International Journal for Numerical and Analytical Methods in Geomechanics* 24 (5):
485 509–29.

486 Hoffmans, G. J., and Verheij, H. J. 1997. *Scour Manual*. CRC Press.

487 Kishore, Y. N., Rao, S. N., and Mani, J. 2008. “Influence of the Scour on Laterally Loaded Piles.” In
488 *The 12th International Conference of International Association for Computer Methods and*
489 *Advances in Geomechanics*.

490 Klinkvort, R. T., and Hededal, O. 2013. “Lateral Response of Monopile Supporting an Offshore
491 Wind Turbine.” *Proceedings of the Institution of Civil Engineers - Geotechnical Engineering*
492 166 (GE2).

493 LeBlanc, C., Houlsby, G. T., and Byrne, B. W. 2010. “Response of Stiff Piles in Sand to Long-Term
494 Cyclic Lateral Loading.” *Géotechnique* 60 (2): 79–90. https://doi.org/10.1680/geot.7.00196.

495 Li, F., Han, J., and Lin, C. 2013. “Effect of Scour on the Behavior of Laterally Loaded Single Piles
496 in Marine Clay.” *Marine Georesources & Geotechnology* 31 (3): 271–89.

497 Li, S., He, S., Li, H. and Jin, Y. 2017. “Scour Depth Determination of Bridge Piers Based on Time-

498 Varying Modal Parameters: Application to Hangzhou Bay Bridge." *Journal of Bridge*
499 *Engineering* 22 (12). https://doi.org/10.1061/(ASCE)BE.1943-5592.0001154.

500 Li, Z., Haigh, S. K., and Bolton, M. D. 2010. "Centrifuge Modelling of Mono-Pile under Cyclic
501 Lateral Loads." In *7th International Conference on Physical Modelling in Geotechnics*, 2:965–
502 70.

503 Liang, F., Zhang, H., and Chen, S. 2018. "Effect of Vertical Load on the Lateral Response of
504 Offshore Piles Considering Scour-Hole Geometry and Stress History in Marine Clay." *Ocean*
505 *Engineering* 158 (April): 64–77. https://doi.org/10.1016/j.oceaneng.2018.03.070.

506 Lin, C., Bennett, C., Han, J., and Parsons, R. L. 2010. "Scour Effects on the Response of Laterally
507 Loaded Piles Considering Stress History of Sand." *Computers and Geotechnics* 37 (7): 1008–
508 14.

509 Lin, C., Han, J., Bennett, C., and Parsons, R. L. 2016. "Analysis of Laterally Loaded Piles in Soft
510 Clay Considering Scour-Hole Dimensions." *Ocean Engineering* 111: 461–70.
511 https://doi.org/10.1016/j.oceaneng.2015.11.029.

512 Maghsoudloo, A., Askarinejad, A., De Jager, R. R., Molenkamp, F., and Hicks, M. A. 2018.
513 "Experimental Investigation of Pore Pressure and Acceleration Development in Static
514 Liquefaction Induced Failures in Submerged Slopes." In *9th International Conference of*
515 *Physical Modelling in Geotechnics*. London, UK.

516 Mostafa, Y. E. 2012. "Effect of Local and Global Scour on Lateral Response of Single Piles in
517 Different Soil Conditions." *Engineering* 4: 297–306.

518 Mu, L., Kang, X., Feng, K., Huang, M., and Cao, J. 2018. "Influence of Vertical Loads on Lateral
519 Behaviour of Monopiles in Sand." *European Journal of Environmental and Civil Engineering*.
520 https://doi.org/10.1080/19648189.2017.1359112.

521 Murphy, G., Igoe, D., Doherty, P., and Gavin, K. 2018. "3D FEM Approach for Laterally Loaded
522 Monopile Design." *Computers and Geotechnics* 100: 76–83.

523 Negro, V., López-Gutiérrez, J. S., Dolores Esteban, M., and Matutano, C. 2014. "Uncertainties in the
524 Design of Support Structures and Foundations for Offshore Wind Turbines." *Renewable Energy*
525 63 (March): 125–32. https://doi.org/10.1016/j.renene.2013.08.041.

526 Nunez, I. L., Hoadley, P. J., and Randolph, M. F. 1988. "Driving and Tension Loading of Piles in
527 Sand on a Centrifuge." In *Proceedings of the International Conference Centrifuge*, 353–62.

528 Peder Hyldal Sørensen, S., and Bo Ibsen, L. 2013. "Assessment of Foundation Design for Offshore
529 Monopiles Unprotected against Scour." *Ocean Engineering* 63 (May): 17–25.
530 https://doi.org/10.1016/j.oceaneng.2013.01.016.

531 Prendergast, L. J., Gavin, K., and Doherty, P. 2015. "An Investigation into the Effect of Scour on the
532 Natural Frequency of an Offshore Wind Turbine." *Ocean Engineering* 101: 1–11.
533 https://doi.org/10.1016/j.oceaneng.2015.04.017.

534 Prendergast, L. J., Hester, D., and Gavin, K. 2016. "Determining the Presence of Scour around
535 Bridge Foundations Using Vehicle-Induced Vibrations." *Journal Of Bridge Engineering* 21
536 (10). https://doi.org/10.1061/(ASCE)BE.1943-5592.0000931.

537 Prendergast, L. J., Reale, C., and Gavin, K. 2018. "Probabilistic Examination of the Change in
538 Eigenfrequencies of an Offshore Wind Turbine under Progressive Scour Incorporating Soil
539 Spatial Variability." *Marine Structures* 57 (January): 87–104.
540 https://doi.org/10.1016/j.marstruc.2017.09.009.

541 Qi, W. G., Gao, F. P., Randolph, M. F., and Lehane, B. M. 2016. "Scour Effects on *p–y* Curves for
542 Shallowly Embedded Piles in Sand." *Géotechnique* 66 (8): 648–60.
543 https://doi.org/10.1680/jgeot.15.P.157.

544 Remaud, D. 1999. “Pieux Sous Charges Latérales: Étude Expérimentale de l’effet de Groupe [Piles
545 under Lateral Loads: Experimental Study of the Group Effect].” Ecole Centrale de Nantes.

546 Robertson, I. N., Riggs, H. R., Yim, S. C., and Young, Y. L. 2007. “Lessons from Hurricane Katrina
547 Storm Surge on Bridges and Buildings.” *Journal of Waterway, Port, Coastal, and Ocean*
548 *Engineering* 133 (6): 463–83.

549 Roulund, A., Sumer, B. M., Fredsøe, J., and Michelsen, J. 2005. “Numerical and Experimental
550 Investigation of Flow and Scour around a Circular Pile.” *Journal of Fluid Mechanics* 534: 351–
551 401.

552 SibelcoEurope. 2016. “Technical Data: Geba Sand.” Eurogrit BV.

553 Sumer, B. M., and Fredsøe, J. 2002. *The Mechanics of Scour in the Marine Environment*. World
554 Scientific.

555 Sumer, B. M., Hatipoglu, F., and Fredsøe, J. 2007. “Wave Scour around a Pile in Sand, Medium
556 Dense, and Dense Silt.” *Journal of Waterway, Port, Coastal, and Ocean Engineering* 133 (1):
557 14–27.

558 Sumer, B. M., Fredsøe, J., and Christiansen, N. 1992. “Scour Around Vertical Pile in Waves.”
559 *Journal of Waterway, Port, Coastal and Ocean Engineering* 118 (1): 15–31.

560 Tokyo Sokki Kenkyujo. 2018. “Strain Gauge Product Information.” 2018.
561 http://web.archive.org/web/20190731182929/https://tml.jp/e/product/strain_gauge.

562 Verdure, L., Garnier, J., and Levacher, D. 2003. “Lateral Cyclic Loading of Single Piles in Sand.”
563 *International Journal of Physical Modelling in Geotechnics* 3 (3): 17–28.

564 Wang, C., Yu, X., and Liang, F. 2017. “A Review of Bridge Scour: Mechanism, Estimation,
565 Monitoring and Countermeasures.” *Natural Hazards* 87 (3): 1881–1906.
566 https://doi.org/10.1007/s11069-017-2842-2.

567 Wind Europe. 2017. “Offshore Wind in Europe - Key Trends and Statistics.”
568 https://doi.org/10.1016/S1471-0846(02)80021-X.

569 Zhang, H., Chen, S., and Liang, F. 2017. “Effects of Scour-Hole Dimensions and Soil Stress History
570 on the Behavior of Laterally Loaded Piles in Soft Clay under Scour Conditions.” *Computers*
571 *and Geotechnics* 84: 198–209. https://doi.org/10.1016/j.compgeo.2016.12.008.

572